olism, positron emission tomography kinetics, and 1-methyl-4-phenyl-1,2,3,6-tetrahydropyridine lesions in primates. *Brain Res.* 1997;750(1–2):264–276.
61. Emborg ME, et al. Age-related declines in nigral neuronal function correlate with motor impairments in rhesus monkeys. *J Comp Neurol.* 1998; 401(2):253–265.
62. Saiki H, Hayashi T, Takahashi R, Takahashi J. Objective and quantitative evaluation of motor function in a monkey model of Parkinson's disease. *J Neurosci Methods.* 2010;190(2):198–204.
63. Någren K, Müller L, Halldin C, Swahn CG, Lehikoinen P. Improved synthesis of some commonly used PET radioligands by the use of [11C] methyl triflate. *Nucl Med Biol.* 1995;22(2):235–239.
64. Herzog H, et al. NEMA NU2-2001 guided performance evaluation of four Siemens ECAT PET scanners. *IEEE Trans Nucl Sci.* 2004;51(5):2662–2669.
65. Gunn RN, Lammertsma AA, Hume SP, Cunningham VJ. Parametric imaging of ligand-receptor binding in PET using a simplified reference region model. *Neuroimage.* 1997;6(4):279–287.
66. Sturgeon C. Practice guidelines for tumor marker use in the clinic. *Clin Chem.* 2002;48(8):1151–1159.
67. Al-Sugair A, Coleman RE. Applications of PET in lung cancer. *Semin Nucl Med.* 1998;28(4):303–319.
68. Nichols TE, Holmes AP. Nonparametric permutation tests for functional neuroimaging: a primer with examples. *Hum Brain Mapp.* 2002;15(1):1–25.
69. Smith SM, Nichols TE. Threshold-free cluster enhancement: addressing problems of smoothing, threshold dependence and localisation in cluster inference. *Neuroimage.* 2009;44(1):83–98.

Cell Transplantation, Vol. 22, pp. 1613–1625, 2013

0963-6897/13 $90.00 + .00
DOI: http://dx.doi.org/10.3727/096368912X658791
E-ISSN 1555-3892
www.cognizantcommunication.com

Transplantation of Bone Marrow Stromal Cell-Derived Neural Precursor Cells Ameliorates Deficits in a Rat Model of Complete Spinal Cord Transection

Misaki Aizawa-Kohama,*† Toshiki Endo,† Masaaki Kitada,* Shohei Wakao,*
Akira Sumiyoshi,‡ Dai Matsuse,* Yasumasa Kuroda,§ Takahiro Morita,*†
Jorge J. Riera,‡ Ryuta Kawashima,‡ Teiji Tominaga,† and Mari Dezawa*§

*Department of Stem Cell Biology and Histology, Tohoku University Graduate School of Medicine, Sendai, Japan
†Department of Neurosurgery, Tohoku University Graduate School of Medicine, Sendai, Japan
‡Institute of Development, Aging and Cancer, Tohoku University, Sendai, Japan
§Department of Anatomy and Anthropology, Tohoku University Graduate School of Medicine, Sendai, Japan

After severe spinal cord injury, spontaneous functional recovery is limited. Numerous studies have demonstrated cell transplantation as a reliable therapeutic approach. However, it remains unknown whether grafted neuronal cells could replace lost neurons and reconstruct neuronal networks in the injured spinal cord. To address this issue, we transplanted bone marrow stromal cell-derived neural progenitor cells (BM-NPCs) in a rat model of complete spinal cord transection 9 days after the injury. BM-NPCs were induced from bone marrow stromal cells (BMSCs) by gene transfer of the Notch-1 intracellular domain followed by culturing in the neurosphere method. As reported previously, BM-NPCs differentiated into neuronal cells in a highly selective manner in vitro. We assessed hind limb movements of the animals weekly for 7 weeks to monitor functional recovery after local injection of BM-NPCs to the transected site. To test the sensory recovery, we performed functional magnetic resonance imaging (fMRI) using electrical stimulation of the hind limbs. In the injured spinal cord, transplanted BM-NPCs were confirmed to express neuronal markers 7 weeks following the transplantation. Grafted cells successfully extended neurites beyond the transected portion of the spinal cord. Adjacent localization of synaptophysin and PSD-95 in the transplanted cells suggested synaptic formations. These results indicated survival and successful differentiation of BM-NPCs in the severely injured spinal cord. Importantly, rats that received BM-NPCs demonstrated significant motor recovery when compared to the vehicle injection group. Volumes of the fMRI signals in somatosensory cortex were larger in the BM-NPC-grafted animals. However, neuronal activity was diverse and not confined to the original hind limb territory in the somatosensory cortex. Therefore, reconstruction of neuronal networks was not clearly confirmed. Our results indicated BM-NPCs as an effective method to deliver neuronal lineage cells in a severely injured spinal cord. However, reestablishment of neuronal networks in completed transected spinal cord was still a challenging task.

Key words: Cell transplantation; Functional magnetic resonance imaging (fMRI); Bone marrow stromal cells (BMSCs); Neural progenitor cells (NPCs); Spinal cord injury (SCI)

INTRODUCTION

Spinal cord injury (SCI) induces local neural cell death and disruption of axonal pathways. Recovery is limited, since the central nervous system (CNS) environment deters axonal growth and regeneration through the actions of myelin inhibitors and astrocytes (14,45). Among the many experimental approaches to treat SCI, cell transplantation has the potential to repair or compensate for local spinal cord damage (5,15,27,32,44).

Bone marrow stromal cells (BMSCs) constitute a possible source of cells for autologous transplantation. They can be obtained from patient bone marrow aspirates and are readily expanded in vitro, which has made them a suitable candidate for clinical applications (9,11,34). We have established a method in which neural progenitor cells can be induced from BMSCs by introduction of the Notch-1 intracellular domain (NICD) followed by culturing using the neurosphere method (10,17). These progenitor cells, that is, bone marrow-derived neural progenitor cells (BM-NPCs), successfully formed spheres that highly expressed markers related to neural progenitors. When BM-NPCs were transplanted into a rat stroke model, they were shown to differentiate into neuronal cells, reconstruct synapses with host neurons, and lead to functional recovery of the animals (17).

Received October 7, 2011; final acceptance August 15, 2012. Online prepub date: October 31, 2012.
Address correspondence to Toshiki Endo, Department of Neurosurgery, Tohoku University Graduate School of Medicine, 1-1 Seiryo, Aoba, 980-8574, Sendai, Japan. Tel: +81-22-717-7230; Fax: +81-22-717-7233; E-mail: endo@nsg.med.tohoku.ac.jp *or* Mari Dezawa, Department of Stem Cell Biology and Histology and Department of Anatomy and Anthropology, Tohoku Univeristy Graduate School of Medicine, 2-1 Seiryo-machi, Aoba-ku, 980-8575, Sendai, Japan. Tel: +81-22-717-8025; Fax: +81-22-717-8030; E-mail: mdezawa@med.tohoku.ac.jp

In the present study, we newly applied BM-NPC transplantation to a rat model of complete spinal cord transection. The aim of this study is to confirm selective neuronal differentiation of the grafted BM-NPCs in the injured spinal cord and to achieve functional recovery. A possible means of achieving recovery from the injury would be the reconstruction of disrupted neuronal circuits between grafted cells and endogenous surrounding neurons, as suggested elsewhere (1). We employed immunohistochemistry to confirm neuronal differentiation of the grafted cells in the injured spinal cord. Synaptic formation of the BM-NPCs was evaluated with synaptophysin and postsynaptic density (PSD)-95. Retrograde tracing with fluorogold (FG) was utilized to see whether the BM-NPCs extended neurites across the transected portion of the spinal cord. We also used functional magnetic resonance imaging (fMRI) of the brain using blood oxygenation level-dependent (BOLD) contrast (12,13,30,40) to test sensory recovery and detect reestablishment of ascending neurotransmission across the injury. Behavioral analysis was included to evaluate locomotor recovery.

MATERIALS AND METHODS

Preparation of Marrow Stromal Cells and Neural Induction

All animal experiments were approved by the Animal Studies Ethics Committee of Tohoku University Graduate School of Medicine. Experimental procedures are presented in Figure 1. Numbers of animals used for each experiment were listed in Table 1. Rat BMSCs were isolated from adult female 10-week-old Wistar rats (CLEA Japan, Inc., Tokyo, Japan) according to methods described previously (4). Cells were maintained in α-minimum essential medium (α-MEM; Sigma, St. Louis, MO, USA) containing 10% fetal calf serum (FCS; Hyclone, Inc., Logan, UT, USA) and kanamycin (Wako Pure Chemical industries, Ltd., Osaka, Japan) at 37°C with 5% carbon dioxide. Next, the cells were transfected with a vector (pCI-neo-NICD) containing the mouse NICD (10). The NICD cDNA coded for a transmembrane region that included a small fragment of extracellular domain followed by a sequence encoding the entire intracellular domain of mouse Notch (initiating at amino acid 1,703 and terminating at the 3′-untranslated sequence).

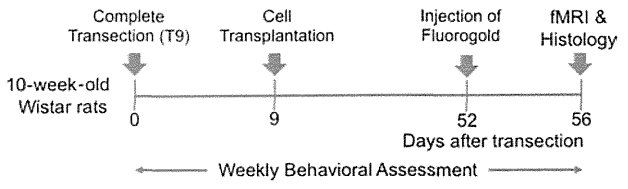

Figure 1. Experimental procedure. See Materials and Methods for detailed information. fMRI, functional magnetic resonance imaging.

Table 1. The Number of Animals per Experiments

	BBB Locomotor Scale	Fluorogold Tracing	fMRI Study	Total
Vehicle group	$n=14$	$n=4$	$n=6$	$n=14$
BM-NPCs group	$n=10$	$n=4$	$n=6$	$n=10$

BBB, Basso, Beattie, Bresnahan; BM-NPCs, bone marrow-derived neural progenitor cells; fMRI, functional magnetic resonance imaging.

This fragment was subcloned into a pCI-neo vector (Promega, Madison, WI, USA) and was transfected with BMSCs using Lipofectamine LTX (Invitrogen, Carlsbad, CA, USA) and selected using G418 (Invitrogen) for 5 days according to the manufacturer's instructions (10).

Induction of BM-NPCs

After G418 selection, rat NICD-transfected cells were washed and cultured in α-MEM containing 10% FCS for 2 days for recovery. The efficacy of NICD transfection was 98.8±0.8%, which is consistent with the previous report (10). During the expansion and recovery of transfected cells after G418 selection, green fluorescent protein (GFP) lentivirus (provided by Dr. D. Trono, Lausanne, Switzerland) was added to the culture medium for labelling purposes (29,39). Efficacy of GFP transfection was calculated three times. After recovery, the cells were washed and cultured in neurobasal medium supplied with B27 supplement (Invitrogen), 20 ng/ml of basic fibroblast growth factor and epidermal growth factor (both R&D Systems, Minneapolis, MN, USA) (17) at a cell density of 100,000 cells/ml on low cell-binding dishes (Nalgene Nunc, Rochester, NY, USA). After 8 days, generated spheres, namely BM-NPCs, were resuspended in Neurobasal medium to a concentration of approximately 30,000 cells/μl and transplanted to the injured rat spinal cord.

Immunocytochemistry

Spheres were fixed with 4% paraformaldehyde in 0.1 mol/L phosphate-buffered saline (PBS; both from Wako Pure Chemical Industries), collected by centrifugation, embedded in optimal cutting temperature (OCT) compound (Sakura Finetek Japan, Tokyo, Japan), and cut into 10-μm-thick sections using a cryostat (CM1850; Leica, Wetzlar, Germany). Samples were incubated with blocking solution containing 5% normal goat serum (Vector Laboratories, Burlingame, CA, USA), 0.1% Triton X-100 (Sigma), and 0.3% bovine serum albumin (BSA; Sigma) in 0.1 mol/L PBS at room temperature for 30 min. Samples were then incubated with primary antibodies in blocking solution overnight at 4°C. After three washes with 0.1 mol/L PBS, samples were incubated with secondary antibodies for 2 h at room temperature, followed by counterstaining with 4′,6-diamidino-2-phenylindole (DAPI) (for nuclear staining,

1:500; Sigma). The following primary antibodies were used for immunocytochemistry: anti-sex-determining region Y box 2 (Sox2; rabbit IgG, dilution 1:5,000; Chemicon, Temecula, CA, USA), anti-neurogenic differentiation (NeuroD; rabbit IgG, 1:200; Chemicon), anti-nestin (mouse IgG, 1:400; BD Pharmingen, San Jose, CA, USA), and anti-musashi (rabbit IgG, 1:200; Millipore, Billerica, MA, USA), anti-neuron-specific nuclear antigen (NeuN) (mouse IgG, 1:200; Chemicon), anti-glial fibrillary acidic protein (GFAP) (mouse IgG, 1:300; Sigma-Aldrich), and anti-oligodendrocyte marker 4 (O4; mouse IgM, 1:20; Millipore). These primary antibodies were detected with Alexa 488-conjugated anti-rabbit IgG or anti-mouse IgG antibodies (Molecular Probes, Invitrogen, Eugene, OR, USA) or Alexa 546-conjugated anti-rabbit IgG (1:500; Molecular Probes) or biotin-conjugated anti-mouse IgM (1:500; Jackson ImmunoResearch, West Grove, PA, USA) and streptavidin Alexa Fluor 488 (1:500; Molecular Probes) and streptavidin Alexa Fluor 680 (1:200; Molecular Probes). Percentages of immunopositive cells were calculated by comparing the cell numbers with the number of DAPI-positive cells. Cells in five fields, each including 100–500 cells, were counted in three independent cultures. Results were averaged and expressed as mean ± SEM.

Complete Transection of the Midthoracic Spinal Cord (T9)

Adult, 10-week-old female Wistar rats weighing 200 ± 20 g underwent complete transection of the spinal cord at the midthoracic level. Under isoflurane anesthesia (Wako Pure Chemical Industries), a laminectomy was performed at the T8–9 level. The spinal cord was exposed and transected completely using microscissors. Possible remaining adhesions were cut with a scalpel, and the rostral and caudal stumps were carefully lifted to verify complete transection. The dural incision was left open. Muscle and skin were sutured separately. The urinary bladder was emptied manually twice daily during the first week and once daily thereafter for 8 weeks.

Transplantation of BM-NPCs

Nine days after SCI rats were randomly assigned to groups receiving vehicle (vehicle group; $n = 14$) or induced neural progenitor cells (BM-NPC group; $n = 10$). Based on a previous report, the timing of transplantation was chosen to avoid delivering cells in an acute inflammatory stage following the injury or in chronic stage in which glial scar tissues would hinder regeneration of axons (31). The numbers of animals used in each experiment are shown in Table 1. Rats were reanesthetized and the thoracic spinal cord was carefully reexposed. Four injections were made with a depth of 1 mm, at 2 mm rostral and caudal of the lesion, and 0.5 mm left and right from the midline. At each site, 2.5 μl of cell suspension or vehicle (α-MEM; Sigma) was infused stereotactically using a Hamilton microsyringe attached to a glass micropipette at the rate of 0.5 μl/min (Hamilton, Reno, NV, USA). A total of 300,000 BM-NPCs were delivered to the spinal cord. The needles were left in the place for 1 min following each injection to prevent cells leaking from the site (2).

Immunohistochemical Analysis

Eight weeks after SCI, animals were anesthetized with an overdose of pentobarbiturate (Wako Pure Chemical Industries) and perfused transcardially with 4% paraformaldehyde in 0.1 mol/L PBS. Spinal cords were removed and embedded in OCT compound, and axial or sagittal slices were cut. Each spinal cord slice was cut into 10-μm sections using a cryostat. In three animals in each group, sagittal sections were used for neurofilament staining. The other immunohistochemical analyses were performed with axial slices. For immunostaining, the sections were washed with PBS and incubated with 5% normal goat serum, 0.3% Triton X-100, and 0.3% BSA in PBS (blocking solution) at room temperature for 30 min to block nonspecific binding. The slides were incubated with primary antibodies diluted in the blocking solution and incubated overnight at 4°C. After three washes with PBS containing 0.05% Triton X-100, the slides were incubated with secondary antibodies for 2 h at room temperature, followed by counterstaining with DAPI, which was diluted in PBS containing 0.1% Triton X-100. Sections were immunolabeled with the following primary antibodies: anti-neuron-specific class III β-tubulin (antibody name: Tuj-1; mouse IgG, 1:200; Sigma-Aldrich), anti-NeuN (mouse IgG, 1:200; Chemicon), anti-GFAP (mouse IgG, 1:300; Sigma-Aldrich), anti-O4 (mouse IgM, 1:20; Millipore), anti-synaptophysin (mouse IgG 1:1000; Chemicon), anti-PSD-95 (mouse IgG2a 1:100; Chemicon), anti-neurofilament (rabbit IgG, 1:200; Chemicon), and anti-GFP (chicken IgG, 1:1,000; Abcam, Philadelphia, PA, USA). Secondary antibodies were anti-mouse Alexa Fluor 568 (1:500; Molecular Probes), biotin-conjugated anti-chicken IgG (1:200; Jackson ImmunoResearch), anti-rabbit Alexa Fluor 568 (1:500; Molecular Probes), and streptavidin Alexa Fluor 488 (1:500; Molecular Probes). After immunolabeling, the samples were inspected under a confocal microscope system (C1si; Nikon, Tokyo, Japan). Using three animals in the BM-NPC group, transplanted cells in 20 fields in each cryosection were counted to confirm the survival of GFP-positive transplanted cells and evaluated the differentiation of BM-NPCs in the injured spinal cord. Results were averaged and expressed as mean ± SEM.

Tracing Study

To label regenerated axons, FG (Fluorochrome, Denver, CO, USA) was injected into the spinal cord 4 days before the rats were killed (41). Using four rats in each group,

4% FG was injected into the spinal cord 10 mm caudal to the transected site over a period of 3 min using a microsyringe (24). After transcardiac perfusion, sections in the axial plane in the thoracic spinal cord including rostral and caudal ends of the transected site, cervical spinal cord, and the brain were stained with anti-FG (rabbit IgG, 1:200; Millipore) as a primary antibody and Alexa 568-conjugated anti-rabbit IgG (1:500, Molecular Probes) as a secondary antibody. Numbers of FG-positive grafted cells were counted at the rostral boundary of the transected spinal cord up to 5 mm from the transected stump. Results were averaged and expressed as mean ± SEM.

Locomotor Scale

Motor function in the hind limbs of all animals ($n=24$) was assessed using the Basso, Beattie, Bresnahan (BBB) locomotor rating scale on the day after injury and each week for 8 weeks after injury (6). Hind limb function was scored from 0 (flaccid paralysis) to 21 (normal gait) as a blind basis. The BM-NPC and vehicle groups were compared using multiple measurement analysis of variance (ANOVA) followed by Tukey's test. All values are given as mean ± SEM. For comparison, we also applied Mann–Whitney U test to evaluate BBB locomotor scale. A value of $p<0.05$ was considered statistically significant.

Functional MRI

Animal Preparation. Rats subjected to spinal cord transection and BM-NPC transplantation ($n=6$) or vehicle injection ($n=6$) underwent brain fMRI 8 weeks after injury, as described (25,40,42). Rats were first anesthetized with isoflurane (2.5% during induction and intubation) mixed with oxygen (30%) and air (70%). Rats were intubated and mechanically ventilated using a rodent ventilator (SAR-830AP Ventilator; CWE, Ardmore, PA, USA). A pair of small needle electrodes (NE-224S; Nihon-Koden, Tokyo Japan) was implanted subcutaneously in the left hind limb of each animal to deliver electrical stimulation. To confirm correct placement of the electrodes, a short sequence of current pulses (0.5 mA) was applied outside the magnet to evoke light muscle twitches. Next, a bolus of α-chloralose (20 mg/kg) (Sigma-Aldrich) was injected through the tail vein catheter, and 10 min later, the isoflurane was discontinued. Anesthesia was continued with α-chloralose infusion (20 mg/kg/h), and pancuronium bromide (2 mg/kg/h; Sigma-Aldrich Japan, Inc., Tokyo, Japan) was added for muscle relaxation. Rectal temperature was monitored and maintained at 37 ± 0.5°C using a water-circulating pad (CLEA Japan, Inc.) during the experiment.

fMRI Recordings. All MRI data were acquired using a 7T Bruker PharmaScan system (Bruker Biospin, Karlsruhe, Germany) with a 38-mm diameter birdcage coil. Prior to all MRI experiments, we first performed global magnetic field shimming inside the core and later completed shimming at the region of interest (ROI) by using a point-resolved spectroscopic protocol (37). Line width (full width at half maximum) at the end of the shimming procedure ranged from 15 to 20 Hz in the ROI (~300 μl). For the rat experiment, BOLD signals were obtained using gradient echo planar imaging (EPI) with the following parameters: repetition time (TR) = 1500 ms, echo time (TE) = 15 ms, spectral band width (SBW) = 250 kHz, field of view (FOV) = 25 × 14 mm^2, matrix size = 125 × 70, number of slices = 7, slice thickness = 1 mm, slice gap = 0 mm, number of volumes = 427, and number of dummy scans = 4.

Electrical Stimulation. A block design paradigm consisting of 10 blocks was employed, in which each block comprised 13 image packages of stimulation followed by 27 image packages of the resting condition. Electrical pulses were produced using a generator (SEN-3401; Nihon Koden) and an isolator (SS-203J, Nihon Koden). Pulsed currents of 10.0 mA with 0.3 ms duration and a constant frequency of 3 Hz were first delivered to the left hind limb of animals.

fMRI Data Analysis. Using statistical parametric mapping software (SPM2, Wellcome Department of Cognitive Neurology, London, UK), we normalized an individual rat's brain to the rat brain atlas template using the T2-weighted images (38). Spatial smoothing was performed using a Gaussian kernel of 0.6 mm full width at half maximum. Single-subject analysis was performed with a critical T value for each voxel calculated for the significance level of $p<0.001$. In response to the hind limb stimulation, volumes of significant clusters in cortex were compared between the groups using the Student's t test, after normal distribution of the data sets were confirmed using Kolmogorov–Smirnov test. We counted fMRI signals in bilateral somatosensory cortex. Activations were counted separately in the hind limb territory of the primary somatosensory cortex as well as the cortical areas medial and lateral to the hind limb area as defined in the rat atlas (36). Time course of BOLD signals (%) was depicted for the BM-NPC transplantation groups using a voxel [2.6, –2.0, –1.0] located in the original hind limb territory of primary somatosensory cortex (36). A single time course was created by averaging across all stimulation periods as described elsewhere (35). All values are given as mean ± SEM.

RESULTS

Grafted BM-NPCs Survived and Differentiated Into Neuronal Lineage Cells in the Injured Spinal Cord

In neurosphere culture, the NICD transfected BMSCs formed spheres. We examined the expression of nestin, NeuroD, Sox2, and musashi to determine whether these

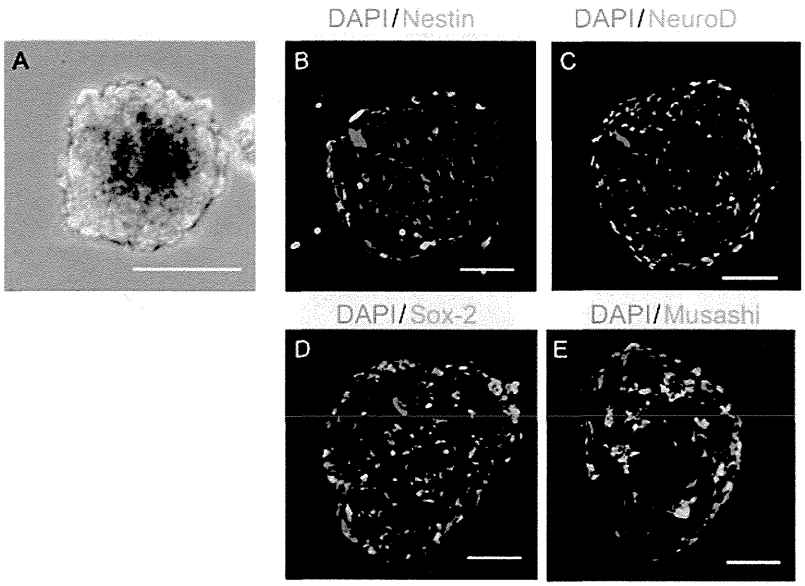

Figure 2. Induction of bone marrow-derived neural progenitor cells (BM-NPCs). (A) A phase contrast microscopy demonstrating BM-NPCs forming spheres on a low cell-binding dish. (B–E) Immunofluorescence images. Expression of nestin (B), neurogenic differentiation (NeuroD) (C), sex-determining region Y box 2 (Sox2) (D), and musashi (E) was confirmed. DAPI, 4′,6-diamidino-2-phenylindole. Scale bars: 50 μm.

spheres contained cells with neural progenitor cell markers. Spheres contained high percentages of cells positive for nestin (62.5±2.1%), NeuroD (82.3±2.1%), Sox2 (87.8±1.4%), and musashi (81.9±1.4%) (Fig. 2), while none of the cells were positive for NeuN (not shown). In addition, spheres did not contain cells positive for GFAP and O4 (not shown) suggesting that, consistent with the previous report, cells committed to the glial fate were not present in the sphere (17,28).

Next, BM-NPCs were transplanted into the injured spinal cord. Over 7 weeks after transplantation, no tumor formation was observed in any of the 10 spinal cords by inspection or histological analysis. Continuity of the spinal cord parenchyma was confirmed macroscopically and by neurofilament immunohistochemistry (Fig. 3A, B). Grafted cells were recognized in vivo by positive labeling of GFP. After transplantation of BM-NPCs 2 mm rostral and caudal to the transected portion of the spinal cord, grafted cells were confirmed to be located as far as 6 mm from the center of the injury (Fig. 3C–F). The total numbers of GFP-labeled cells were $8.02\pm0.71\times10^3$ in the injured spinal cord. Efficacy of GFP transfection was 45.0±4.4% in vitro. Accurate assessment of donor cell survival can only be pursued by counting all of the GFP signals in every spinal cord section. In this sense, there is a limitation of assessing the true measure of donor cell survival in our count, but the ratio of transplanted cells that survived in the injured spinal cord was estimated to be roughly 5.9%.

Importantly, BM-NPCs survived and showed low capacity for differentiating into astrocytes in the injured spinal cord. The frequencies of βIII tubulin (antibody Tuj-1)- and NeuN-positive cells among GFP-positive cells were 77.2±2.6% (Fig. 4A–E) and 36.0±3.2% (Fig. 4F–I), respectively. Nestin-positive cells were observed among the GFP-positive cells at the ratio of 9.7±2.0% (Fig. 4J–M), while the ratio of GFAP-positive cells was 2.9±0.9% (Fig. 4N–Q). O4 positive cells could not be detected (not shown). These observations suggested that the majority of the transplanted BM-NPCs became neuronal marker-positive cells. Moreover, the frequency of nestin-positive cells, which was 62.5±2.1% in vitro and 9.7±2.0% in vivo, indicated advancement of differentiation of the transplanted cells within the injured spinal cord, as nestin is potential indicator of neural differentiation (43). Spheres contained no cells positive for NeuN, while the frequency of NeuN-positive cells among GFP-positive cells increased in vivo, which also supported differentiation of the grafted cells. Transplanted cells were also found to express the synaptic marker synaptophysin (Fig. 5). Among GFP-positive cells, 24.2±2.2% were positive for synaptophysin. It was noted that synaptophysin was localized predominantly next to GFP-positive transplanted cells in a punctate pattern (Fig. 5). To further assess the synaptic formation between the transplanted cells and the host cells, immunohistochemistry for PSD-95 was performed (8,22). PSD-95 labeling was adjacent to the synaptophysin-positive signal in the transplanted cells (Fig. 6).

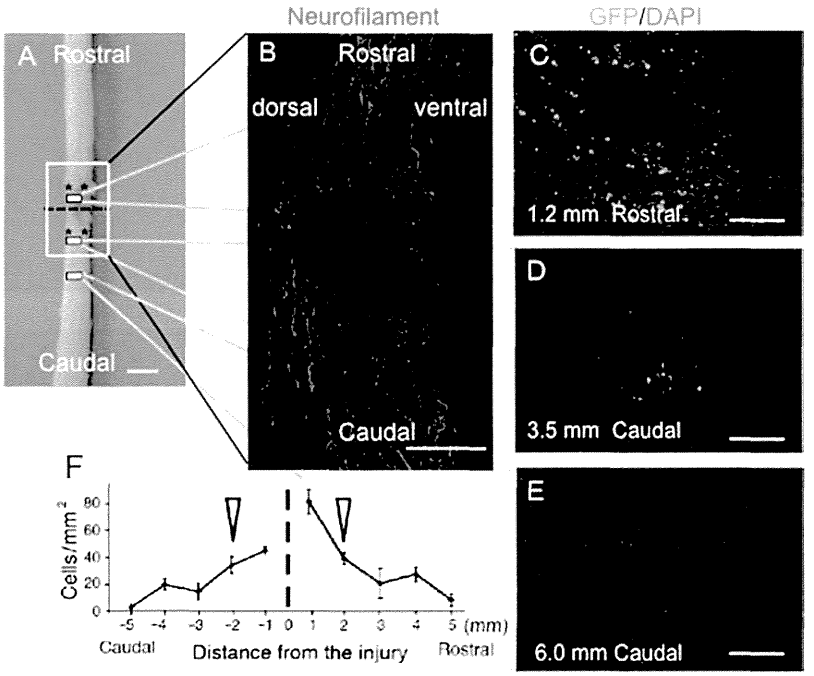

Figure 3. Transplanted bone marrow-derived neural progenitor cells (BM-NPCs) in the injured spinal cord 8 weeks after transection. (A) Schematic drawing of a representative spinal cord from the BM-NPC group showing sites of transection (dotted line) and transplantation (*). (B) Representative longitudinal section stained for neurofilaments corresponding to the white box in (A), showing anatomical continuity of spinal cord parenchyma at the injury site. (C–E) Distribution of green fluorescent protein (GFP)-positive transplanted cells at sites 1.2 mm rostral (C), 3.5 mm caudal (D), and 6.0 mm caudal (E) to the injury center in the dorsal spinal cord. Positions of the panels are indicated by small boxes in (A). (F) Numbers of GFP-positive cells between 5 mm caudal and 5 mm rostral to the injury center. The dotted line and arrowheads indicate the transected portion and the site of cell transplantation, respectively. Note that the GFP-positive cells were incorporated into the host spinal cord. DAPI, 4′,6-diamidino-2-phenylindole. Scale bars: 2 mm (A), 250 μm (B), 100 μm (C–E).

Fluorogold Tracing Detected Extension of Neurites From BM-NPCs Across the Transected Site in the Spinal Cord

Four days before the animals were sacrificed, we injected the retrograde tracer FG 10 mm caudal to the transected site, so that FG would be taken up through the terminals of the regenerated neurites (Fig. 7A). Strikingly, in the BM-NPC group, we detected FG-labeled grafted cells in the rostral as well as caudal spinal cord in all four rats (Fig. 7B–G). The presence of cells double positive for FG and GFP rostral to the transected portion indicated that the grafted cells extended their neurites across the transected portion to reach the caudal spinal cord. The site of injection was carefully examined to ensure that no FG could have reached the transected portion by diffusion (24). The number of cells labeled with FG and GFP at the rostral boundary of the transected spinal cord was $5.17 \pm 0.75/mm^2$ in the BM-NPC group. FG-labeled BM-NPCs were located rostrally 1.8 ± 0.18 mm from the transection stump to a maximum of 4.6 mm. In the vehicle group, no FG-labeled cells were found in the spinal cord rostral to the transected site. In any of the injured animals with or without treatments ($n=4$, each group), no FG-labeled cells were found in the cervical spinal cord or in the brain sections.

Behavioral Analysis Indicated Improved Hind Limb Locomotor Function After BM-NPC Transplantation

BBB locomotor scores for the BM-NPC and vehicle groups were determined each week for 8 weeks after injury (Fig. 8). Improvements in hind limb motor function were significantly greater in the BM-NPC group than in the vehicle group after 2 weeks ($p<0.01$) and over 3–8 weeks ($p<0.001$, repeated measures ANOVA followed by post hoc Tukey's test). Mann–Whitney U test also indicated significant functional recovery between 2 and 8 weeks (Fig. 8). Eight weeks after the injury, averaged BBB scale of injured animals was 3.31 in the control group while 5.80 in BM-NPCs transplantation group. Following the treatments, rats showed symptoms of recovery; they showed extensive movements of the three joints in the hind limbs. The difference between these groups was statistically significant ($p<0.001$, post hoc Tukey's test; $p<0.01$, Mann–Whitney U test).

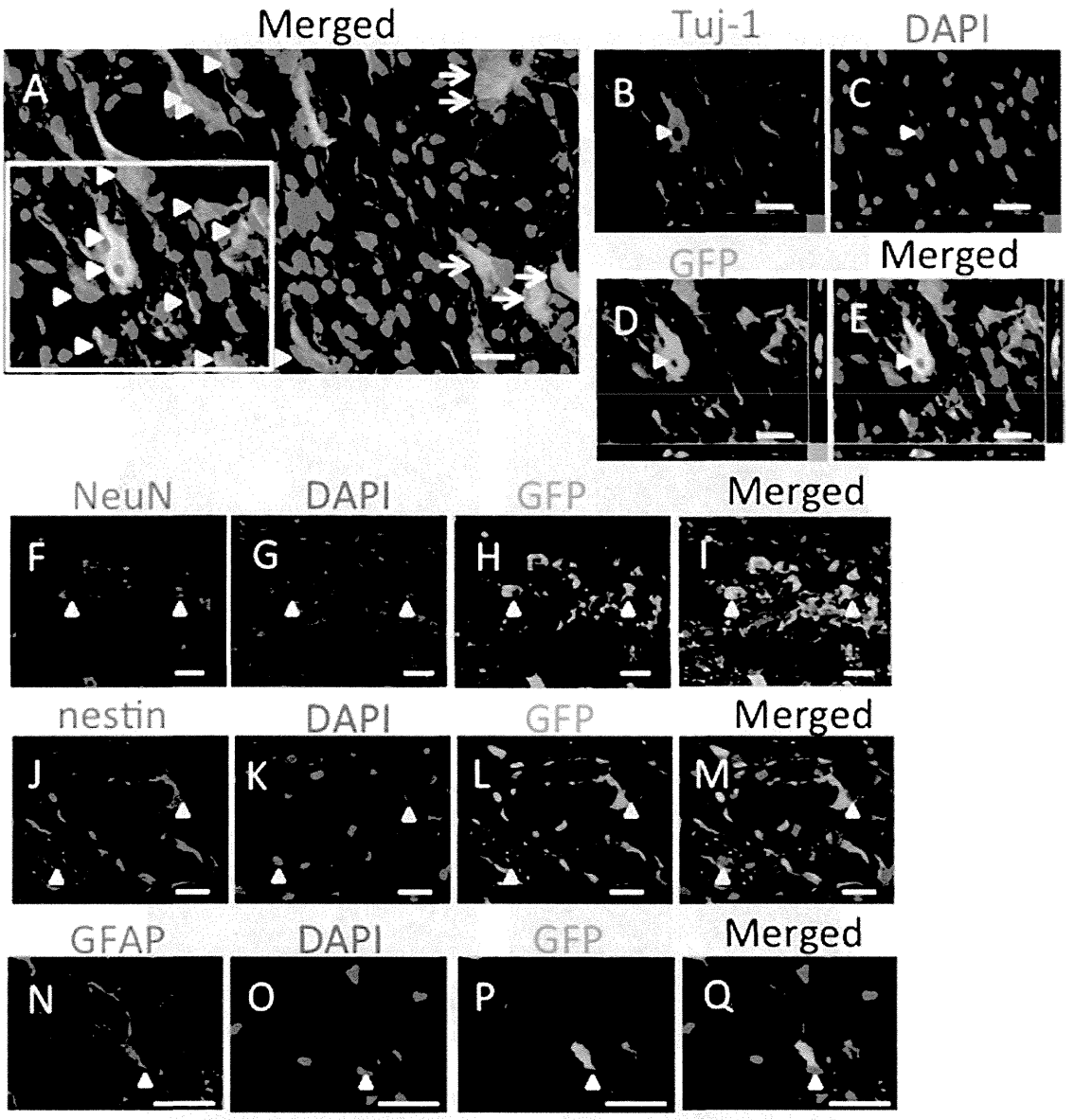

Figure 4. Differentiation of green fluorescent protein (GFP)-positive bone marrow-derived neural progenitor cells (BM-NPCs) in the spinal cord 8 weeks after injury. (A–Q) Cells labeled with neuron-specific class III β-tubulin (antibody: Tuj-1) (A–E) and neuronal nuclei (NeuN) (F–I) were encountered more frequently than those labeled with nestin (J–M) or glial fibrillary acidic protein (GFAP) (N–Q). Arrowheads, positively labeled cells. Arrows, GFP-positive and Tuj-1-negative cells. DAPI, 4′,6-diamidino-2-phenylindole. Scale bars: 20 μm.

Functional MRI Was Not Able to Provide Evidence of Reconstruction of Local Neuronal Networks After BM-NPC Transplantation

In response to electrical stimulation to the hind limbs, we counted fMRI signals in the bilateral somatosensory cortex in both BM-NPC and vehicle groups. BOLD signal changes were as high as 2.4% in the original hind limb territory in the BM-NPC group (Fig. 9). In the contralateral hind limb territory (HL) as defined in Figure 9B (36), volumes of activation in the BM-NPC group were significantly larger than those in the vehicle group ($p=0.014$, Student's t test) (Fig. 9C). Particularly, we noticed that cortical activation in spinally injured rats was not confined to the original hind limb territory in the primary somatosensory cortex (Fig. 9D). Signals extended more medially and even to the ipsilateral side of stimulation. Total volumes of cortical activation were 1.53 ± 0.83 and 0.41 ± 0.17 mm^3 in the BM-NPC and vehicle groups, respectively, while the difference was not statistically significant ($p=0.11$, Student's t test).

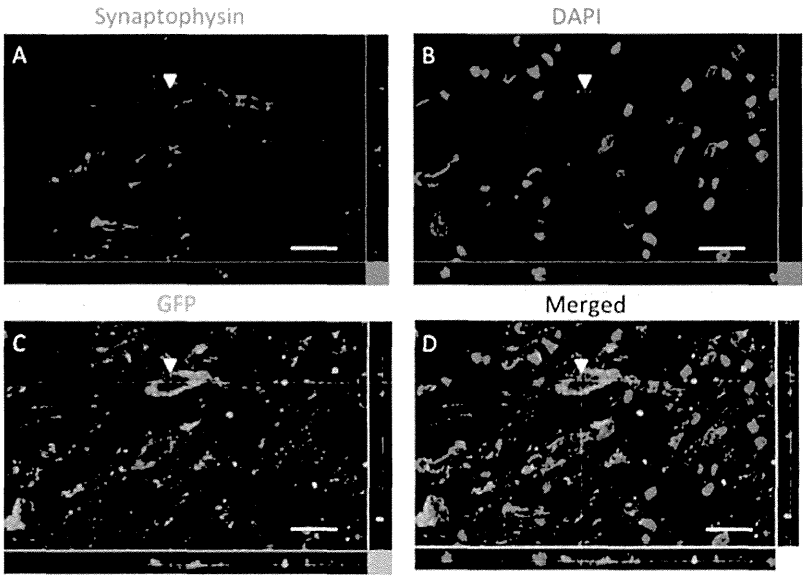

Figure 5. Synaptophysin expressed around GFP-positive bone marrow-derived neural progenitor cells (BM-NPCs). Photomicrographs depicting synaptophysin (A), DAPI (B), GFP (C), and a merged image (D) staining of transplanted cells in the spinal cord. This finding suggests the synapse formation between the transplanted cells and host cells. Arrowheads indicate positively labeled cells. Abbreviations are as in Figure 4. Scale bars: 20 μm.

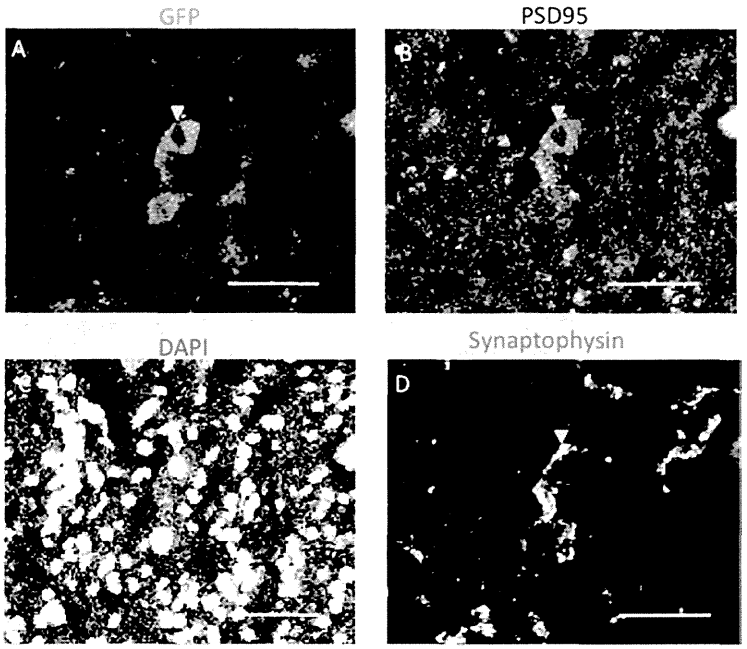

Figure 6. Postsynaptic density (PSD-95) localized adjacent to synaptophysin on GFP-positive bone marrow-derived neural progenitor cells (BM-NPCs). Photomicrographs depicting GFP (A), PSD-95 (B), DAPI (C), and synatophysin (D) staining of cells in the spinal cord. This finding suggests synapse formation between the transplanted cells and host cells. Arrowheads indicate positively labeled cells. Abbreviations are as in Figure 4. Scale bars: 50 μm.

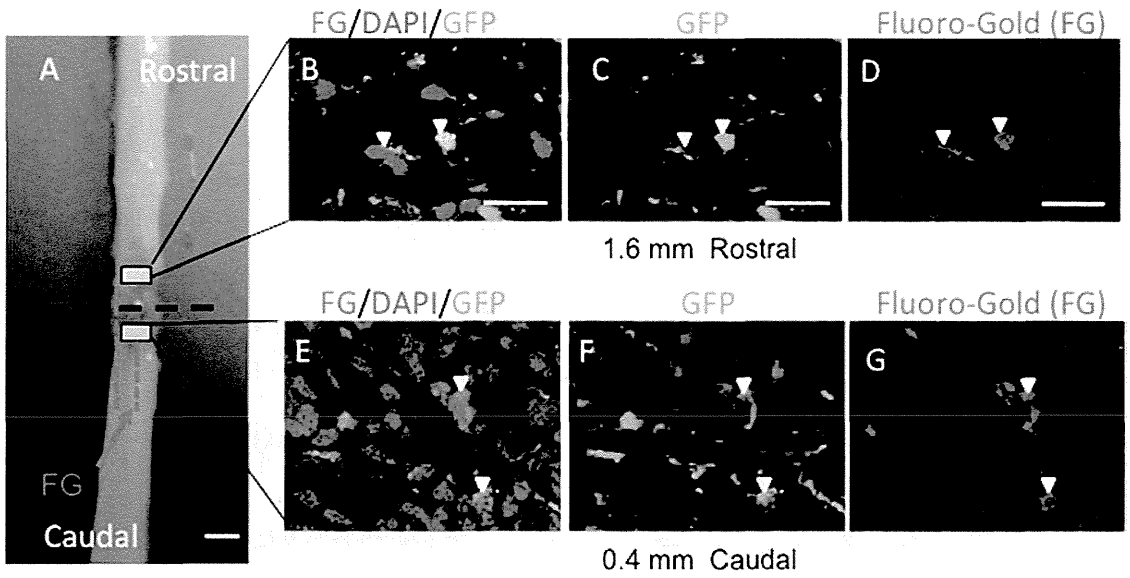

Figure 7. Expression of the retrograde tracer Fluorogold (FG) injected 10 mm caudal to the transected site of the spinal cord. (A) Schematic drawing of a representative spinal cord taken from the bone marrow-derived neural progenitor cell (BM-NPC) group, showing sites of FG injection (red arrow). Red dotted lines indicate the supposed routes by which FG was transported from the terminals of extended neurites and crossed the transected portion. (B–G) Green fluorescent protein (GFP)-positive BM-NPCs, transplanted rostral (B–D) and caudal (E–G) to the injured site, were also positive for FG in representative sections obtained 1.6 mm rostral and 0.4 mm caudal to the transected site. Abbreviations, schematic drawings, and arrowheads are as described in Figures 2 and 3. Scale bars: 2.0 mm (A) and 20 μm (B–G).

DISCUSSION

In this study, we report that transplantation of BM-NPCs promoted functional recovery of the spinally injured animals evidenced by improved locomotor scores. The grafted cells survived and committed predominant neuronal differentiation in the injured spinal cord. Immunohistochemistry using synaptophysin and PSD-95 as well as the FG tracing indicated synaptic formation of the BM-NPCs with the surrounding neurons and extension of the neurites across the transected portion in the spinal cord. As a consequence, neuronal networks were partially restored 7 weeks posttransplantation, which was represented as increased cortical signals in fMRI of the BM-NPC transplanted animals. However, the representation of the cortical signals was diverse and altered when compared to the original sensory map. Therefore, reestablishment of neuronal networks by transplantation of BM-NPCs was not fully accomplished.

Here, we demonstrated that transplantation of BM-NPCs was an efficient method in supplying neuronal lineage cells in a severely injured spinal cord. Majority of sphere-derived cells cultured with several trophic factors were reported to express neuronal markers such as βIII tubulin (Tuj-1) and microtubule associated protein 2 in a high ratio

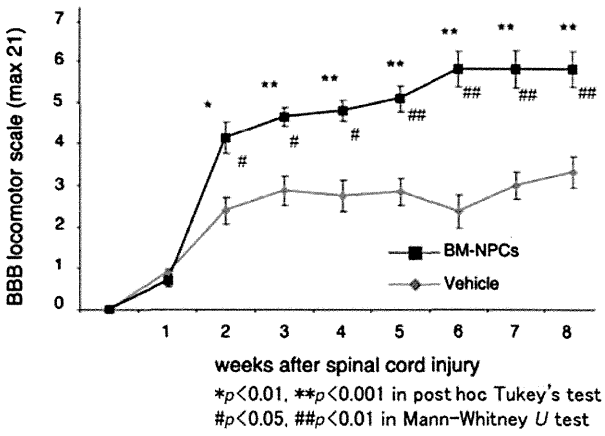

Figure 8. Basso, Beattie, Bresnahan (BBB) locomotor scale. Open-field locomotor hind limb function of all rats was tested on the day after injury and then weekly for 8 weeks postoperatively. Results are shown separately for groups transplanted on day 9 with bone marrow-derived neural progenitor cells (BM-NPCs) ($n=10$) or injected with vehicle ($n=14$). Repeated measures ANOVA followed by the post hoc Tukey's test as well as Mann–Whitney U test showed significant differences between the groups. Two weeks after injury, BBB scores of the BM-NPC group were significantly higher than those of the vehicle group. $*p<0.01$, $**p<0.001$ post hoc Tukey's test. $\#p<0.05$, $\#\#p<0.01$ Mann–Whitney U test.

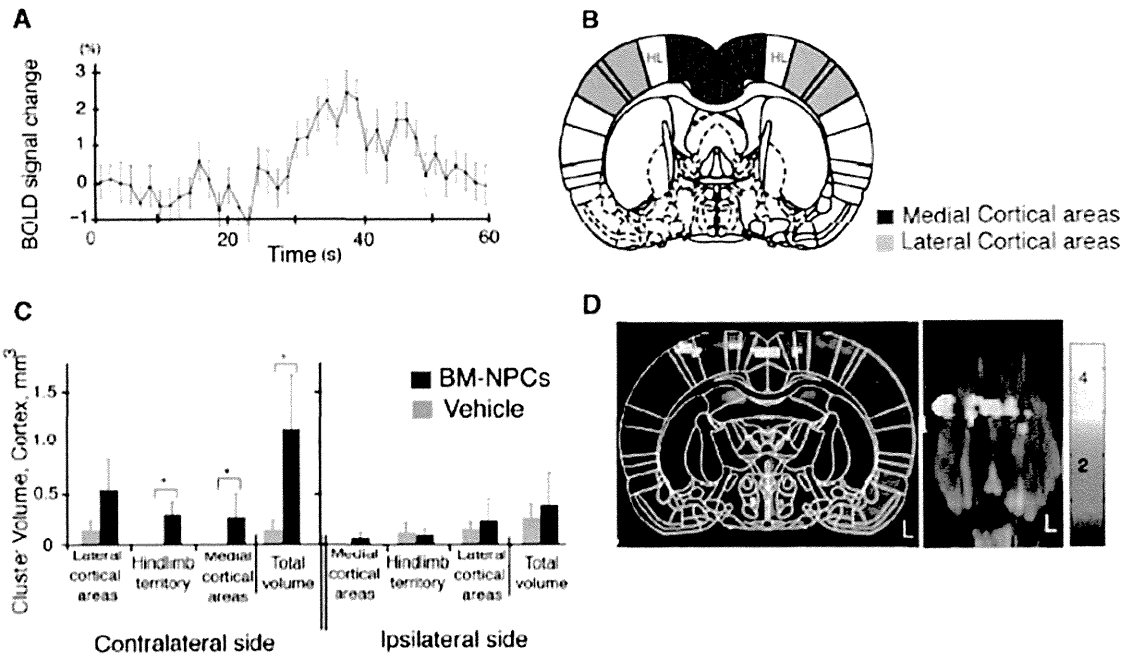

Figure 9. Cortical fMRI signals in response to hind limb stimulation 8 weeks after spinal cord transection. (A) Time course of blood oxygenation level-dependent (BOLD) signals (%) in a voxel in the original hind limb territory in the bone marrow-derived neural progenitor cell (BM-NPC) transplantation group ($n=6$). Gray bars indicate the period of stimulation. (B) Schematic drawing of a rat brain to illustrate medial cortical areas (dark gray), the hind limb territory of the primary somatosensory cortex area (HL) and lateral cortical areas (light gray), in which cortical activations were counted. (C) Volumes of functional magnetic resonance imaging (fMRI) signals in vehicle and BM-NPC groups. Significant differences between the BM-NPC and vehicle injection groups were noted in the signals in the contralateral cortex and the hind limb territory of the contralateral side to the stimulation ($^*p<0.05$). Note that broad cortical areas were activated in response to hind limb stimulation 8 weeks after spinal cord injury. (D) A representative cortical sensory map from the BM-NPCs group, demonstrating neuronal activation in various cortical areas outside of the original hind limb territory in the primary somatosensory cortex. Signals were observed on the left side (L), which was ipsilateral to the stimulation as demonstrated in a coronal section (left) at bregma −1.4 mm and a horizontal section (right). The color scale indicates T statistics calculated by statistical parametric mapping software (SPM2). The coronal sections are superimposed on a schematic brain section from the same level [reproduced with permission of Elsevier from the Paxinos and Watson atlas (36)].

(98.5% and 95.7%, respectively) and GFAP in a low ratio (0.7%) (17). These findings clearly indicated that cells in the BM-NPC-derived spheres tended to differentiate into neurons and were not initially committed to the glial fate. In the same study in which BM-NPC-derived spheres were transplanted into the rat stroke model, BM-NPCs predominantly differentiated into NeuN-expressing postmitotic neurons (79.5%), and only a small population of the transplanted cells expressed GFAP (1.9%) (17). In the present study, we found that the rate of the differentiation of the transplanted GFP-positive cells into the neuronal fate detected by Tuj-1-positive cells was 77.2%; however, that of postmitotic neurons positive for NeuN was only 36.0%. The rate of differentiation into GFAP-positive astrocytes was 2.9%, similar to that observed in the transplantation into the rat stroke model. These observations indicate that, although the ratio of the differentiation into postmitotic neurons was dependent on the disease models, the BM-NPC-derived sphere cells predominantly differentiate into the neuronal fate after transplantation.

In general, the environment of the spinal cord is not permissive for survival and neuronal differentiation of the transplanted cells (19,27). Exogenous neural stem cells undergo proliferation and differentiate mainly into astrocytes in the spinal cord (33). When naive neural stem cells were transplanted into the injured spinal cord, 84% of the cells were GFAP-positive 9 weeks after transplantation, while only 4% of the cells had neuronal characteristics (18). Even when cells are shown to differentiate into neuronal lineage cells in vitro, the degree of neural induction in vivo may turn out to be less than expected after transplantation into the injured spinal cord (7). Our findings indicate that BM-NPCs are a reliable source of neuronal cells that can be used in cell transplantation therapy for SCI. Previously, we transplanted BM-NPCs and naive BMSCs in a rat stroke model and compared the results (17), in which BM-NPCs demonstrated much higher efficacy in survival, differentiation, and integration into the host brain. Having established the difference between BM-NPCs and naive BMSCs, we solely used BM-NPCs in the current protocol.

As Abematsu et al. demonstrated recently, grafted neuronal cells may establish neuronal connectivity by making synaptic connections with endogenous surrounding neurons (1). In this study, immunohistochemistry for synaptophysin and PSD-95 revealed the adjacent localization of synaptophysin and PSD-95 in the same GFP-positive transplanted cells (Fig. 6). Synaptophysin and PSD-95 are markers for presynaptic vesicles and postsynaptic density, respectively, suggesting that the transplanted cells constructed synaptic connections and received synaptic inputs from host and/or surrounding neurons.

In our model, retrograde axonal tracing showed the presence of cells double positive for FG and GFP in the spinal cord rostral to the transected portion. However, no FG-positive cells were detected in cervical spinal cord or brain sections, when we performed histological analyses 4 days following the injection of FG. In a previous report using a matrix seeded with BMSCs to fill the gap of the spinal cord transection injury, FG-labeled neurons were detected in the cortex and in the brainstem a week after the FG injection (22). With regard to the time between the FG injections and histological analyses, 4 days might not be long enough for the retrograde tracers to reach the brain stem through the severely injured spinal cord. Therefore, the purpose of the FG tracing was focused on evaluating grafted BM-NPCs located rostral to the transected stump. To avoid confusion in interpreting results, we only injected FG caudally and 10 mm from the stump. In this way, we could minimize the possibility that the tracer would diffuse and go across the transected portion (22). Results of the FG thus indicated that the grafted cells survived, differentiated, and might have extended neurites across the transected portion of the spinal cord.

Furthermore, the FG-labeled BM-NPCs localized 4.6 mm rostral to the spinal cord stump. Recently, we demonstrated the capacity of migration of BM-NPCs in a rat model of stroke (17). In spinal cord, various studies using in vivo MRI tracking systems have observed that the transplanted cells could actually migrate long distances. In one of these study, injected live cells traveled as far as 9 mm in 8 weeks following the transplantation (23). Although it is possible that dispersion might have transferred the grafted cells a few millimeters, the aforementioned information suggested that the BM-NPCs had the capacity to migrate in the spinal cord.

In this study, transplantation of BM-NPCs to the completely transected adult rat spinal cord led to a significant, albeit modest improvement of hind limb motor function as determined by BBB scoring. Eight weeks after the injury, the BBB score of injured animals was 3.3 without BM-NPC transplantation, while with the transplantation, it improved to 5.8. In other studies, BMSC-derived Schwann cells or olfactory mucosa were transplanted into similar complete spinal cord transection models in Wistar rats. In those studies, BBB scores were 3.6 and 2.6 in the controls, while 7.0 and 4.6 in the treatment groups, respectively (3,20). Degrees of improvement in BBB scores by BM-NPC transplantations were therefore comparable to those of the other studies. Importantly, to judge degrees of locomotor recovery by the BBB scores needs caution, since functional improvement may also depend on the strains used or the types of treatments applied. For instance, in Sprague–Dawley strains, BBB scores were lower and between 0 and 2 following complete transection of the spinal cord (13,26,41). In one of these studies, 10 weeks posttransplantation of olfactory ensheathing cells, BBB scores improved to 4.3 from 1.0 (26).

FMRI also demonstrated an increase of BOLD signals in cortex cerebri in response to electrical stimulation of a hind limb. In particular, cortical activations were not only observed in the original somatosensory cortex, rather the BOLD signals had an abnormal and diverse distribution, including ipsilateral activity. Together, the addition of the BM-NPCs to the injury area might lead to the reestablishment of a degree of ascending and descending neurotransmission across injury, while we could not confirm reconstruction of the disrupted neuronal networks by the distribution of recovered cortical activations in fMRI.

One of the reasons for such ambiguity could partly rely on the end point of this study, which was 7 weeks posttransplantation. In the current methods, we set the end point mainly based on the time course of locomotor recovery. As shown in Figure 8, BBB scores improved and reached a plateau 5–6 weeks after the transplantation. In another experiment using fMRI to evaluate sensory recovery in a rat model of SCI, fMRI was performed 9 weeks posttransplantation, which demonstrated recovery of cortical responses (18). Moreover, in our previous experiment applying BMSC-derived Schwann cells to a rat model of complete spinal cord transection, it was 6 weeks posttransplantation when the axonal regeneration was histologically confirmed (20). However, as we demonstrated previously, reorganization in cerebral cortex may take place over 6 months long after SCI (13). After severe thoracic SCI, cortical connections from the spared forelimbs expanded and took over the deafferented hind limb areas (13,16). If such deafferentation plasticity occurs, the corresponding somatosensory cortex may no longer be available to receive or process recovered ascending sensory information. In this sense, the time allowed for recovery following the complete transection could be too short and limit the value of fMRI in this study.

Another possible explanation for the diverse cortical signals in fMRI is misdirection of sensory inputs through the reconstructed neuronal networks. After transplantation of BM-NPCs, new synaptic pathways relaying peripheral inputs to cortical areas were formed in the injured spinal cord. However, they could be different from those in the original ascending tracts. In such a situation, recovered

sensory inputs would not connect with the original hind limb territory, but with various cortical areas.

Besides specific neuronal cell induction, another possible strategy for treating SCI includes transduction of neural stem cells into the oligodendrocytic lineage to enhance myelination (18,21). Using this approach, myelination of spared axons led to recovery of conduction velocity and promoted functional recovery in SCI. Hypothetically, however, if axons are completely severed in the damaged spinal cord, as occurs in our injury model and a model used by others (1), enhancement of myelination with oligodendrocytes may have limited effectiveness. In this situation, a strategy in which added neuronal cells may serve as a form of interneuron providing a link across the injury may be a more reliable approach. Depending on the degree of injury, one may need to select or combine different types of cell transplantation to achieve the best functional recovery.

We conclude that delayed grafting of BM-NPCs into the injured spinal cord was effective in providing neuronal lineage cells. If an efficient neuronal induction in the injured spinal cord was feasible, reconstruction of disrupted neuronal circuits between grafted cells and endogenous surrounding neurons can be a possible means of achieving recovery from SCI. Depending on the degrees of SCI, we can select or combine different types of cell transplantation to achieve the best functional recovery in SCI and other neural degenerative diseases occurring in the spinal cord.

ACKNOWLEDGMENTS: We thank Ms. Ryoko Mamiya for her technical assistance and Dr. Mitsunobu Matsubara and Dr. Kuniyasu Niizuma (Tohoku University) for their useful inputs to our project. This work was supported by Program for Promotion of Fundamental Studies in Health Sciences of the National Institute of Biomedical Innovation (NIBIO). This work was supported by Program for Promotion of Fundamental Studies in Health Sciences of the National Institute of Biomedical Innovation (NIBIO). The authors declare no conflict of interest.

REFERENCES

1. Abematsu, M.; Tsujimura, K.; Yamano, M.; Saito, M.; Kohno, K.; Kohyama, J.; Namihira, M.; Komiya, S.; Nakashima, K. Neurons derived from transplanted neural stem cells restore disrupted neuronal circuitry in a mouse model of spinal cord injury. J. Clin. Invest. 120:3255–3266; 2010.
2. Ankeny, D. P.; McTigue, D. M.; Jakeman, L. B. Bone marrow transplants provide tisssue protection and directional guidance for axons after contusive spinal cord injury in rats. Exp. Neurol. 190:17–31; 2004.
3. Aoki, M.; Kishima, H.; Yoshimura, K.; Ishihara, M.; Ueno, M.; Hata, K.; Yamashita, T.; Iwatsuki, K.; Yoshimine, T. Limited functional recovery in rats with complete spinal cord injury after transplantation of whole-layer olfactory mucosa: Laboratory investigation. J. Neurosurg. Spine 12: 122–130; 2010.
4. Azizi, S. A.; Stokes, D.; Augelli, B. J.; DiGirolamo, C.; Prockop, D. J. Engraftment and migration of human bone marrow stromal cells implanted in the brains of albino rats—similarities to astrocyte grafts. Proc. Natl. Acad. Sci. USA 95(7):3908–3913; 1998.
5. Baptiste, D. C.; Fehlings, M. G. Update on the treatment of spinal cord injury. Prog. Brain Res. 161:217–233; 2007.
6. Basso, D. M.; Beattie, M. S.; Bresnahan, J. C. A sensitive and reliable locomotor rating scale for open field testing in rats. J. Neurotrauma 12:1–21; 1995.
7. Cao, Q. L.; Howard, R. M.; Dennison, J. B.; Whittemore, S. R. Differentiation of engrafted neuronal-restricted precursor cells is inhibited in the traumatically injured spinal cord. Exp. Neurol. 177:349–359; 2002.
8. Cheng, C.; Gao, S.; Zhao, J.; Niu, S.; Chen, M.; Li, X.; Qin, J.; Shi, S.; Guo, Z.; Shen, A. Spatiotemporal patterns of postsynaptic density (PSD)-95 expression after rat spinal cord injury. Neuropathol. Appl. Neurobiol. 34:340–356; 2007.
9. Dezawa, M.; Hoshino, M.; Nabeshima, Y.; Ide, C. Marrow stromal cells: Implications in health and disease in the nervous system. Curr. Mol. Med. 5:723–732; 2005.
10. Dezawa, M.; Kanno, H.; Hoshino, M.; Cho, H.; Matsumoto, N.; Itokazu, Y.; Tajima, N.; Yamada, H.; Sawada, H.; Ishikawa, H.; Mimura, T.; Kitada, M.; Suzuki, Y.; Ide, C. Specific induction of neuronal cells from bone marrow stromal cells and application for autologous transplantation. J. Clin. Invest. 113:1701–1710; 2004.
11. Ding, D. C.; Shyu, W. C.; Lin, S. Z. Mesenchymal stem cells. Cell Transplant. 20:5–14; 2011.
12. Endo, T.; Spenger, C.; Hao, J.; Tominaga, T.; Wiesenfeld-Hallin, Z.; Olson, L.; Xu, X. J. Functional MRI of the brain detects neuropathic pain in experimental spinal cord injury. Pain 138:292–300; 2008.
13. Endo, T.; Spenger, C.; Tominaga, T.; Brene, S.; Olson, L. Cortical sensory map rearrangement after spinal cord injury: fMRI responses linked to Nogo signalling. Brain 130:2951–2961; 2007.
14. Filbin, M. T. Myelin-associated inhibitors of axonal regeneration in the adult mammalian CNS. Nat. Rev. Neurosci. 4:703–713; 2003.
15. Fitch, M. T.; Silver, J. CNS injury, glial scars, and inflammation: Inhibitory extracellular matrices and regeneration failure. Exp. Neurol. 209:294–301; 2008.
16. Ghosh, A.; Haiss, F.; Sydekum, E.; Schneider, R.; Gullo, M.; Wyss, M. T.; Mueggler, T.; Baltes, C.; Rudin, M.; Weber, B.; Schwab, M. E. Rewiring of hindlimb corticospinal neurons after spinal cord injury. Nat. Neurosci. 13:97–104; 2010.
17. Hayase, M.; Kitada, M.; Wakao, S.; Itokazu, Y.; Nozaki, K.; Hashimoto, N.; Takagi, Y.; Dezawa, M. Committed neural progenitor cells derived from genetically modified bone marrow stromal cells ameliorate deficits in a rat model of stroke. J. Cereb. Blood Flow Metab. 29:1409–1420; 2009.
18. Hofstetter, C. P.; Holmstrom, N. A.; Lilja, J. A.; Schweinhardt, P.; Hao, J.; Spenger, C.; Wiesenfeld-Hallin, Z.; Kurpad, S. N.; Frisen, J.; Olson, L. Allodynia limits the usefulness of intraspinal neural stem cell grafts; directed differentiation improves outcome. Nat. Neurosci. 8:346–353; 2005.
19. Johnson, P. J.; Tatara, A.; Shiu, A.; Sakiyama-Elbert, S. E. Controlled release of neurotrophin-3 and platelet-derived growth factor from fibrin scaffolds containing neural progenitor cells enhances survival and differentiation into neurons in a subacute model of SCI. Cell Transplant. 19: 89–101; 2010.
20. Kamada, T.; Koda, M.; Dezawa, M.; Yoshinaga, K.; Hashimoto, M.; Koshizuka, S.; Nishio, Y.; Moriya, H.; Yamazaki, M. Transplantation of bone marrow stromal cell-derived Schwann cells promotes axonal regeneration and functional recovery after complete transection of adult rat spinal cord. J. Neuropathol. Exp. Neurol. 64:37–45; 2005.

21. Keirstead, H. S.; Nistor, G.; Bernal, G.; Totoiu, M.; Cloutier, F.; Sharp, K.; Steward, O. Human embryonic stem cell-derived oligodendrocyte progenitor cell transplants remyelinate and restore locomotion after spinal cord injury. J. Neurosci. 25:4694–4705; 2005.
22. Kosacka, J.; Nowicki, M.; Kacza, J.; Borlak, J.; Engele, J.; Borowski, K. S. Adipocyte-derived angiopoietin-1 supports neurite outgrowth and synaptogenesis of sensory neurons. J. Neurosci. Res. 83:1160–1169; 2006.
23. Lee, I. H.; Bulte, J. W.; Schweinhardt, P.; Douglas, T.; Trifunovski, A.; Hofstetter, C.; Olson, L.; Spenger, C. In vivo magnetic resonance tracking of olfactory ensheathing glia grafted into the rat spinal cord. Exp. Neurol. 187:509–516; 2004.
24. Liang, H.; Liang, P.; Xu, Y.; Wu, J.; Liang, T.; Xu, X. DHAM-BMSC matrix promotes axonal regeneration and functional recovery after spinal cord injury in adult rats. J. Neurotrauma 26:1745–1757; 2009.
25. Lilja, J.; Endo, T.; Hofstetter, C.; Westman, E.; Young, J.; Olson, L.; Spenger, C. Blood oxygenation level-dependent visualization of synaptic relay stations of sensory pathways along the neuroaxis in response to graded sensory stimulation of a limb. J. Neurosci. 26:6330–6336; 2006.
26. Lu, J.; Feron, F.; Mackay-Sim, A.; Waite, P. M. Olfactory ensheathing cells promote locomotor recovery after delayed transplantation into transected spinal cord. Brain 125:14–21; 2002.
27. Ma, Y. H.; Zhang, Y.; Cao, L.; Su, J. C.; Wang, Z. W.; Xu, A. B.; Zhang, S. C. Effect of neurotrophin-3 genetically modified olfactory ensheathing cells transplantation on spinal cord injury. Cell Transplant. 19:167–177; 2010.
28. Matsuse, D.; Kitada, M.; Ogura, F.; Wakao, S.; Kohama, M.; Kira, J.; Tabata, Y.; Dezawa, M. Combined transplantation of bone marrow stromal cell-derived neural progenitor cells with a collagen sponge and basic fibroblast growth factor releasing microspheres enhances recovery after cerebral ischemia in rats. Tissue Eng. Part A 17:1993–2004; 2011.
29. Nguyen, T. H.; Khakhoulina, T.; Simmons, A.; Morel, P.; Trono, D. A simple and highly effective method for the stable transduction of uncultured porcine hepatocytes using lentiviral vector. Cell Transplant. 14:489–496; 2005.
30. Ogawa, S.; Menon, R. S.; Tank, D. W.; Kim, S. G.; Merkle, H.; Ellermann, J. M.; Ugurbil, K. Functional brain mapping by blood oxygenation level-dependent contrast magnetic resonance imaging. A comparison of signal characteristics with a biophysical model. Biophys. J. 64:803–812; 1993.
31. Okano, H.; Ogawa, Y.; Nakamura, M.; Kaneko, S.; Iwanami, A.; Toyama, Y. Transplantation of neural stem cells into the spinal cord after injury. Semin. Cell. Dev. Biol. 14:191–198; 2003.
32. Olson, L. Regeneration in the adult central nervous system: Experimental repair strategies. Nat. Med. 3:1329–1335; 1997.
33. Parr, A. M.; Kulbatski, I.; Tator, C. H. Transplantation of adult rat spinal cord stem/progenitor cells for spinal cord injury. J. Neurotrauma 24:835–845; 2007.
34. Parr, A. M.; Tator, C. H.; Keating, A. Bone marrow-derived mesenchymal stromal cells for the repair of central nervous system injury. Bone Marrow Transplant. 40:609–619; 2007.
35. Pawela, C. P.; Biswal, B. B.; Hudetz, A. G.; Li, R.; Jones, S. R.; Cho, Y. R.; Matloub, H. S.; Hyde, J. S. Interhemispheric neuroplasticity following limb deafferentation detected by resting-state functional connectivity magnetic resonance imaging (fcMRI) and functional magnetic resonance imaging (fMRI). Neuroimage 49:2467–2478; 2010.
36. Paxinos, G.; Watson, C. The rat brain in stereotaxic coordinates, the new coronal set, fifth ed. New York: Academic Press; 2005.
37. Sanganahalli, B. G.; Bailey, C. J.; Herman, P.; Hyder, F. Tactile and non-tactile sensory paradigms for fMRI and neurophysiologic studies in rodents. Methods. Mol. Biol. 489:213–242; 2009.
38. Schweinhardt, P.; Fransson, P.; Olson, L.; Spenger, C.; Andersson, J. L. A template for spatial normalisation of MR images of the rat brain. J. Neurosci. Methods 129:105–113; 2003.
39. Shimizu, S.; Kitada, M.; Ishikawa, H.; Itokazu, Y.; Wakao, S.; Dezawa, M. Peripheral nerve regeneration by the in vitro differentiated-human bone marrow stromal cells with Schwann cell property. Biochem. Biophys. Res. Commun. 359:915–920; 2007.
40. Spenger, C.; Josephson, A.; Klason, T.; Hoehn, M.; Schwindt, W.; Ingvar, M.; Olson, L. Functional MRI at 4.7 tesla of the rat brain during electric stimulation of forepaw, hindpaw, or tail in single- and multislice experiments. Exp. Neurol. 166:246–253; 2000.
41. Steward, O.; Sharp, K.; Selvan, G.; Hadden, A.; Hofstadter, M.; Au, E.; Roskams, J. A reassessment of the consequences of delayed transplantation of olfactory lamina propria following complete spinal cord transection in rats. Exp. Neurol. 198:483–499; 2006.
42. Sumiyoshi, A.; Riera, J. J.; Ogawa, T.; Kawashima, R. A mini-cap for simultaneous EEG and fMRI recording in rodents. Neuroimage 54:1951–1965; 2011.
43. von Bohlen Und Halbach, O. Immunohistological markers for staging neurogenesis in adult hippocampus. Cell Tissue Res. 329:409–420; 2007.
44. Wang, G.; Ao, Q.; Gong, K.; Zuo, H.; Gong, Y.; Zhang, X. Synergistic effect of neural stem cells and olfactory ensheathing cells on repair of adult rat spinal cord injury. Cell Transplant. 19:1325–1337; 2010.
45. Yiu, G.; He, Z. Glial inhibition of CNS axon regeneration. Nat. Rev. Neurosci. 7:617–627; 2006.

Research article

Treatment with basic fibroblast growth factor-incorporated gelatin hydrogel does not exacerbate mechanical allodynia after spinal cord contusion injury in rats

Takeo Furuya[1], Masayuki Hashimoto[1], Masao Koda[1], Atsushi Murata[1], Akihiko Okawa[1], Mari Dezawa[2], Dai Matsuse[2], Yasuhiko Tabata[3], Kazuhisa Takahashi[1], Masashi Yamazaki[1]

[1]Department of Orthopaedic Surgery, Chiba University Graduate School of Medicine, Chiba, Japan, [2]Department of Anatomy and Neurobiology, Tohoku University Graduate School of Medicine, Sendai, Japan, [3]Department of Biomaterials, Institute for Frontier Medical Sciences, Kyoto University, Kyoto, Japan

Besides stimulating angiogenesis or cell survival, basic fibroblast growth factor (bFGF) has the potential for protecting neurons in the injured spinal cord.

Objective: To investigate the effects of a sustained-release system of bFGF from gelatin hydrogel (GH) in a rat spinal cord contusion model.

Methods: Adult female Sprague–Dawley rats were subjected to a spinal cord contusion injury at the T10 vertebral level using an IH impactor (200 kdyn). One week after contusion, GH containing bFGF (20 μg) was injected into the lesion epicenter (bFGF – GH group). The GH-only group was designated as the control. Locomotor recovery was assessed over 9 weeks by Basso, Beattie, Bresnahan rating scale, along with inclined plane and Rota-rod testing. Sensory abnormalities in the hind paws of all the rats were evaluated at 5, 7, and 9 weeks.

Results: There were no significant differences in any of the motor assessments at any time point between the bFGF – GH group and the control GH group. The control GH group showed significantly more mechanical allodynia than did the group prior to injury. In contrast, the bFGF – GH group showed no statistically significant changes of mechanical withdrawal thresholds compared with pre-injury.

Conclusion: Our findings suggest that bFGF-incorporated GH could have therapeutic potential for alleviating mechanical allodynia following spinal cord injury.

Keywords: Allodynia, Basic fibroblast growth factor, Scaffold, Spinal cord injuries, Motor deficits, Neuroprotection, Locomotor recovery, Paraplegia

Introduction

Spinal cord injury (SCI) is the most devastating type of trauma for patients due to the long-lasting disability and limited responses to acute drug administration and efforts at rehabilitation. Previously, we reported on combinational therapy, bone marrow stromal cell (BMSC) transplantation, and Rho-kinase inhibitor administration for spinal cord contusion.[1] Combination therapy showed better recovery than controls, but we detected no synergy between the components of the combination. We counted lower numbers of remaining BMSCs and saw a gradual decrease in the number of BMSCs over the observation period. We hypothesized that we might have observed more locomotor recovery had the remaining cells been more abundant.

Gelatin hydrogel (GH) incorporating basic fibroblast growth factor (bFGF) is one of the more promising tools for treating SCI. bFGF-incorporated GH has enhanced angiogenesis in several experimental models,[2–4] and it has already found some clinical

Correspondence to: Masayuki Hashimoto, Department of Orthopaedic Surgery, Chiba University Graduate School of Medicine, 1-8-1 Inohana, Chuo-ku, Chiba 260-8670, Japan. Email: futre@tg7.so-net.ne.jp

DOI 10.1179/2045772312Y.0000000030

usage, including a phase I/IIa study in humans in the hope of enhancing angiogenesis.[5] Multiple studies have also identified various functions for bFGF itself in damaged central nerve system tissue, including the following: attenuating neurotoxicity and increasing antioxidant enzyme activities in hippocampal neurons;[6] protecting against excitotoxicity and chemical hypoxia in both neonatal and adult rat neurons;[7] preventing the death of lesioned cholinergic neurons *in vivo*;[8] and protecting spinal motor neurons after experimental SCI.[9] These research findings together suggest that bFGF-incorporated GH has the potential for saving damaged neuronal cells and improving angiogenesis after SCI.

BMSC with fibrin scaffolding has been observed to improve survival of transplanted cells after spinal cord hemisection.[10] The combination of the neurotrophin-3, platelet-derived growth factor, and fibrin scaffold has been reported to enhance the total number of neural progenitor cells present in the spinal cord lesion 2 weeks after injury.[11] The study findings together suggest that the controlled release of growth factor incorporated into a scaffold in conjunction with cell transplantation has the potential to improve the survival of transplanted cells and enhancing locomotor recovery after SCI.

In the present study, we sought to establish the safety of bFGF-incorporated GH in humans. Our study protocol was to inject bFGF-incorporated GH and GH without bFGF into contused spinal cords in rats and to measure locomotion for 9 weeks after SCI, as well to estimate two types of allodynia before and after SCI.

Methods

Experimental groups

The 18 animal subjects were randomly assigned to two groups: (1) the bFGF + GH group (bFGF – GH, $n = 8$), which received an injection of bFGF + GH mixture into the spinal cord; (2) the GH-only group (GH, $n = 10$), which received an injection of GH without bFGF into the spinal cord.

bFGF-incorporated GH treatment

bFGF-incorporated GH

A frozen aliquot of bFGF (10 μg/μl) was diluted 1:1 with phosphate-buffered saline (PBS) and incubated overnight at 4°C (5 μg/μl). GH (2 mg) was mixed with a 20-μl aliquot of bFGF and incubated at 37°C for 1 hour. Just before injection, bFGF-incorporated GH was diluted by 20 μl of PBS. We injected 8 μl bFGF-incorporated GH into the injured spinal cord.

Animal surgery

Our experimental SCI protocol utilized a total of 18 8-week-old female Sprague–Dawley rats (SLC, Hamamatsu, Japan). Rats were anesthetized with 1.6% halothane in 0.5 l/minute oxygen. We performed a laminectomy at the T9–T10 levels and induced a contusion injury of the spinal cord with the infinite horizon impactor (IH impactor, 200 kdyn, Precision Systems and Instrumentation, Lexington, NY, USA). Rats were group-housed in the animal facility and maintained under conditions of constant temperature and humidity. Food and water were provided *ad libitum*. Manual bladder expression was performed twice a day until recovery of the bladder reflex. All animals were given antibiotics (500 μl/day; Bactramin, Chugai Pharmaceutical, Tokyo, Japan) by subcutaneous administration once a day for 3 days. Body weight after SCI was measured weekly, from which we calculated body weight ratios by dividing each post-injury body weight by the body weight before surgery.

Seven days after injury, we re-exposed the injury site and injected the same volume (8 μl) of bFGF-incorporated GH, or GH only, into the center of the injured spinal cord using a micro-glass pipette needle attached to a 10-μl Hamilton syringe (Hamilton Company, Reno, NV, USA) under microscopy. We performed the injection at multiple depths (2, 1.5, 1.0, and 0.5 mm) during drawback, and the needle was left in the spinal cord for 3 minutes following the last injection in order to minimize reflux. None of the animals showed abnormal behavior. All the experimental procedures were performed in compliance with the guidelines established by the Animal Care and Use Committee of Chiba University.

Assessments of sensory motor functions

Basso, Beattie, Bresnahan open field locomotor test

Hind limb function was assessed in an open field (100 cm × 60 cm plastic pool) using the Basso, Beattie, Bresnahan (BBB) open field locomotor test.[12] Measurements were performed weekly thereafter for 9 weeks. Tests were videotaped for 5 minutes and scored by a trained observer who was unaware of the treatment group to which each subject was assigned.

Inclined plane test

Each animal was placed in head-up, transverse, and head-down positions on an inclined plane and the angle of slope gradually increased. The angle at which the animal fell down from the slope was recorded for each position, two trials per animal, after SCI. The better of the two trial results for each subject were

combined and compared among the three groups. We performed these measurements before surgery and then 4, 6, and 8 weeks after SCI.

Rota-rod test

Four and 6 weeks after SCI, animals were placed on a 5 cm-wide turning cylinder (Rota-rod MK-630B, Muromachi Kikai, Japan) and forced to walk on it. The speed of rotation was gradually accelerated from 3 rpm (rotations per minute) to 30 rpm, and then maintained at 30 rpm for 5 minutes (Mode A1, 3–30 rpm). The time when the animal fell from the Rota-rod was recorded. Preoperatively, animals were able to stay on the Rota-rod for a mean duration of 199.3 seconds.

Sensory tests

Thermal nociceptive thresholds in rat hind limbs were evaluated using a Hargreaves device (Ugo Basile, Varese, Italy). The rats were placed in individual transparent acrylic boxes with the floor maintained at 28°C. A heat stimulus (150 mcal/seconds/cm^2) was delivered using a 0.5 cm-diameter radiant heat source positioned under the plantar surface of the hind limb. The heat source was placed alternately under each hind limb to avoid anticipation by the animal. A cutoff time of 22 seconds was used, as we had previously ascertained that no tissue damage would result within this time period. The withdrawal threshold was calculated as the average value of three consecutive tests. Mechanical withdrawal thresholds in rat hind limbs were tested using a dynamic plantar aesthesiometer (Ugo Basile), in which a mechanical stimulus was applied via an actuator filament (0.5 mm diameter), which under computer control applied a linear ramp 5.0 g/seconds to the plantar surface of the hind limb. The withdrawal threshold was calculated as the average of six consecutive tests. Both tests were performed pre-injury and then 5, 7, and 9 weeks after contusion.

Anterograde labeling of the cortico-spinal tract with biotinylated dextran amine; immunohistochemical; and histological assessments

Nine weeks after contusion, the cortico-spinal tract was bilaterally traced under halothane anesthesia with 2.0 µl biotinylated dextran amine (BDA, molecular weight: 10 000, 10% in 0.01 M PBS, Molecular Probes, Carlsbad, CA). A micro-glass pipette needle attached to a 2-µl Hamilton syringe was stereotaxically guided, and BDA was slowly injected into four sites in the sensorimotor cortex for the hind limb at a 1-mm depth: Bregma 2 mm, sagittal suture 2 mm; Bregma 2 mm, sagittal suture 3 mm; Bregma 2.5 mm, sagittal suture 3 mm; Bregma 2.5 mm, sagittal suture 2.5 mm. The needle was left in place for 1 minute following each injection to minimize reflux.

Histology

Animals were subjected to trans-cardiac perfusion with 4% paraformaldehyde in PBS (pH 7.4) 14 days after BDA injection. The spinal cords were dissected and immersed overnight in 4% paraformaldehyde and then stored in 20% sucrose in PBS. The spinal cords were cut into 20-mm lengths (10 mm rostral to and 10 mm caudal to the lesion site) and embedded in optimal cutting temperature (OCT) compound (Tissue Tek, Sakura Finetechnical, Tokyo, Japan). We sectioned each block in the sagittal plane (25 µm) using a cryostat and mounted eight consecutive sections on poly-L-lysine-coated slides (Matsunami, Tokyo, Japan) to make serial sections. The sections on each slide were sliced at 150 µm intervals; each eight section slide therefore covered approximately 1200 µm of the lesion site. We performed histological or immunohistochemical staining on the slides.

To evaluate lesion size, we stained three slices from each animal with cresyl violet. We determined the cavity size of each section using Photoshop 5.5 software (Adobe, San Jose, CA, USA). We calculated a mean cavity size from these three values for each animal and compared cavity sizes between groups.

For anterograde labeling of the cortico-spinal tract with BDA, sections were incubated with Alexa Fluor 594-conjugated streptavidin (1:800; Molecular Probes). We selected seven consecutive sections from the rostral edge of the lesion center, which we photographed with a 20× objective lens using a fluorescence microscope (DP71, Olympus, Tokyo, Japan). We added up the number of fibers and compared the fiber counts between the groups.

Three slices per animal, centered on the lesion epicenter, were incubated with rabbit anti-calcitonin gene-related peptide (CGRP) antibody (1:1000, ImmunoStar, Inc. Hudson, WI, USA) or rabbit anti-von Willebrand factor (1:400, Dako Cytomation, Glostrup, Denmark), then reacted with Alexa-Fluor 594 goat anti-rabbit IgG secondary antibody. Slices were photographed on the rostral and caudal edges of the lesion epicenter with a 10× objective lens using a fluorescence microscope (DP71, Olympus). The numbers of CGRP-positive immunoreactive fibers or von Willebrand factor-positive immunoreactive vessels were counted and averaged.

Statistical analysis

For histological studies and for assessments of sensory motor functions at each time point, we performed a

Mann–Whitney *U* test. For the 9-week locomotor scale, we performed repeated-measures analysis of variance (ANOVA). Data were reported as mean values ± SEM. Differences with *P* values <0.05 were considered statistically significant.

Results

We measured body weight ratios every week after SCI. Rats were treated with bFGF – GH, or GH, 7 days after SCI. Weight loss was severe at 7 days after SCI: weight loss ratios for the bFGF – GH and the GH groups were 0.958 ± 0.020 and 0.938 ± 0.013, respectively. At the end of 9 weeks, the weights of the animals had increased to 1.322 ± 0.039 and 1.319 ± 0.034, respectively, for two groups. No statistically significant increase in the body weight ratio was observed during the entire experiment.

BBB locomotor scores 7 days after SCI were 1.0 ± 0.49 and 0.6 ± 0.34, respectively, for the bFGF – GH and the GH groups, and the intergroup difference was not statistically significant. BBB scores at 9 weeks were 10.5 ± 0.54 and 10.2 ± 0.58, respectively, for the two groups, and again no statistically significant difference between the groups was observed (Fig. 1). Repeated-measures ANOVA also failed to detect any statistically significant intergroup differences in BBB scores over the entire experiment period ($P = 0.27$).

Inclined plane testing showed that before SCI, rats could keep their body on an inclined plane at 61.04 ± 0.43° in a head-up position, 57.29 ± 0.44° in a transverse position, and 45.83 ± 0.25° in a head-down position. The differences were not statistically significant between groups at 4, 6, and 8 weeks after SCI (data not shown). The Rota-rod test also showed no statistically significant differences between groups at 4, 6, and 8 weeks after SCI (data not shown).

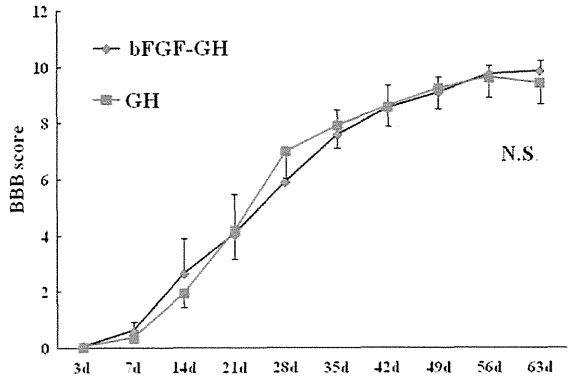

Figure 1 BBB locomotor scores during the first 9 weeks after SCI. The differences between the groups were not statistically significant ($P = 0.27$).

Analysis of the pre-injury data for the Hargreaves device revealed a mean thermal latency of 16.9 ± 0.4 seconds ($n = 18$). Thermal latency decreased to mean values of 13.5 ± 0.9 seconds at 5 weeks, 14.7 ± 1.0 seconds at 7 weeks, and 14.0 ± 1.1 seconds at 9 weeks in the bFGF – GH group, and 13.2 ± 1.0 seconds at 5 weeks, 13.9 ± 0.9 seconds at 7 weeks, and 13.4 ± 0.7 seconds at 9 weeks in the GH group. Although thermal latency decreased in both groups after SCI compared with normal pre-injury rats, the differences did not reach statistical significance. In addition, none of the differences in mean thermal latency between the groups at any time period were statistically significant.

Mechanical thresholds using a dynamic plantar aesthesiometer had a mean pre-injury value of 31.5 ± 1.4 g (Fig. 2: $n = 18$). The mean values decreased to 26.2 ± 1.5 g at 5 weeks, 27.2 ± 1.2 g at 7 weeks, and 28.5 ± 1.9 g at 9 weeks in the bFGF – GH group, and 22.9 ± 2.1 g at 5 weeks, 25.2 ± 2.0 g at 7 weeks, and 28.5 ± 2.2 g at 9 weeks in the GH group. The GH group exhibited significantly more mechanical allodynia compared with pre-injury rats at 5 and 7 weeks ($P = 0.006$ and $P = 0.021$, respectively). The decreases in mechanical thresholds in the bFGF – GH group were not statistically significant over the course of the entire experiment.

To elucidate the efficacy of bFGF – GH or GH for tissue protection or tissue sparing after SCI, we measured the area of the cystic cavity with cresyl violet staining 9 weeks after injury (Fig. 3). The differences between the groups did not reach statistical significance (Fig. 3C, $P = 0.94$).

The BDA signals rostral to the lesion epicenter were 49.1 ± 13.7 and 38.9 ± 11.9 for the bFGF – GH and GH groups, respectively (Fig. 4). The differences

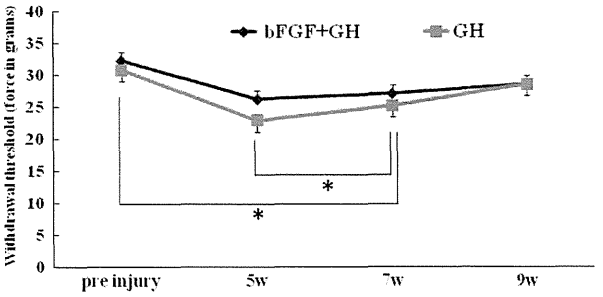

Figure 2 Mechanical thresholds using a dynamic plantar aesthesiometer were performed pre-injury and also 5, 7, and 9 weeks after contusion. The GH group showed significantly more mechanical allodynia compared with pre-injury rats at 5 and 7 weeks ($P = 0.006$ and $P = 0.021$, respectively). However, the bFGF – GH group showed no statistically significant decrease over the entire experiment.

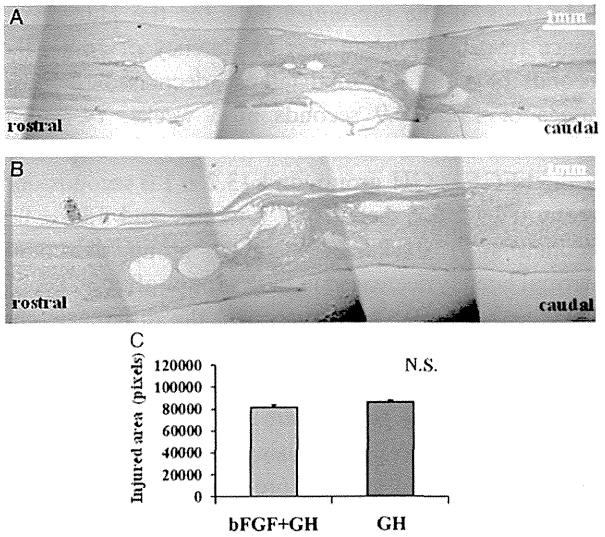

Figure 3 Cresyl violet staining 9 weeks after SCI did not show statistically significant cavity size differences between the two groups. The cavity size of each section was analyzed. Representative figures of each group from the bFGF + GH group (A) and the GH group (B) are presented. The differences among groups did not reach statistical significance (C, $P = 0.94$). Bar = 1 mm for figures A, B.

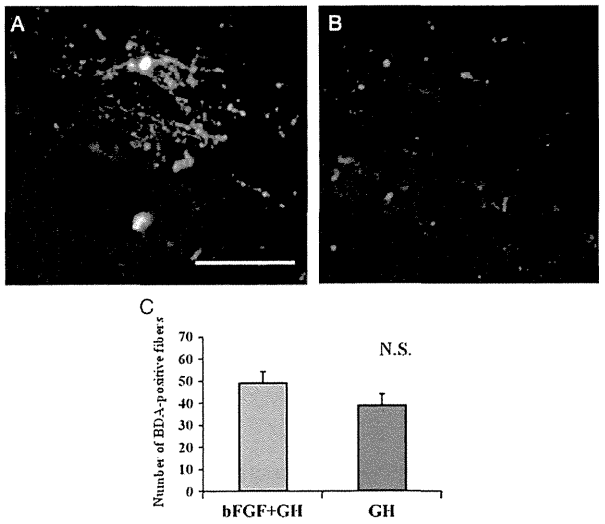

Figure 4 Biotinylated dextran amine tracing 8 weeks after SCI. The BDA signals at the rostral edge of the lesion epicenter were analyzed. The differences between the groups did not reach statistical significance (C, $P = 0.22$). Bar = 100 μm for figures A, B.

between the two groups did not reach statistical significance (Fig. 4C, $P = 0.22$). In the same way, we analyzed von Willebrand factor-positive signals at the lesion epicenter. Values were 23 ± 12.0, and 17.6 ± 5.2, for the bFGF – GH and GH groups, respectively. No statistically significant difference between groups was observed ($P = 0.83$).

The CGRP signals from the posterior funiculus on the rostral and caudal sides of the lesion epicenter were analyzed and compared. CGRP-positive fiber counts were 7.1 ± 2.6 and 35.2 ± 6.5 for the bFGF–GH and GH groups, respectively, and none of the differences were statistically significant ($P = 0.17$).

Discussion

Although we injected bFGF-incorporated GH 1 week after SCI in our experimental model, the optimal timing of bFGF injection remains an unresolved issue. Several studies, though, have provided suggestive data. For instance, one study detected significant increases in various molecular forms of FGF2 protein 4 days after SCI.[13] Another study showed significant up-regulation of bFGF 3 days after SCI, when cell proliferation is maximal.[14] A third study tracked bFGF mRNA, which initially was detected 1 hour post-injury, increased between 6 hours and 3 days, declined thereafter, and returned to baseline levels by 21 days.[15] These reports together indicate that up-regulation of bFGF is maximal 3 days after SCI and gradually decreases after that, from which we deduce that in terms of timing, it is best to wait until after bFGF up-regulation has peaked before injecting bFGF. Furthermore, another study showed that epidermal growth factor and FGF2 injection immediately after SCI had no impact on BBB scores for 8 weeks.[16] On the basis of all these studies, we decided to inject bFGF-incorporated GH 7 days after SCI.

We measured BBB scores for 9 weeks after SCI and also performed Rota-rod and inclined plane testing at several time points after SCI. The locomotor measurement data showed no statistically significant recovery in this study. bFGF – GH and GH-only injections appear to have had almost identical effects on injured spinal cords. In other words, both the bFGF – GH and the GH injections may have improved the ability of injured rats to perform weight-bearing activity. While the saline-injected SCI model rats that suffered the same contusion injury of the spinal cord did not reach weight-bearing levels in their BBB scores in our previous study,[1] rats of both groups in this study were able to perform weight-bearing activity. This result implies the possibility that GH itself has neuroprotective effects. Further investigation is needed to clarify this point. To examine associated histological changes, we assessed cortico-spinal tract tracing 2 weeks before sacrifice. Comparisons of BDA signals did not show statistically significant differences between groups. This histological finding supports the locomotor assessments in which bFGF

– GH and GH-only injections showed no statistically significant recovery in this study.

We measured two types of allodynia using a Hargreaves device and a dynamic plantar aesthesiometer. We observed no statistically significant differences between groups and in comparison with pre-injury rats, in mean thermal latency using the Hargreaves device. With respect to mechanical allodynia using the dynamic plantar aesthesiometer, while the GH injection group showed significantly more mechanical allodynia than the pre-injury data, the bFGF – GH group showed no statistically significant threshold changes compared with pre-injury. Although no statistically significant differences in the posterior funiculus CGRP-positive fiber counts between rostral and caudal sides of the lesion epicenter were observed, CGRP-positive fiber counts were lower in the bFGF – GH group. The histology data thus show some correspondence with the mechanical allodynia testing data, i.e. the bFGF – GH injection group had significantly less sensitivity to mechanical allodynia.

Conclusion

To summarize, the findings of this study revealed that the bFGF – GH group showed no statistically significant threshold changes compared with pre-injury, whereas the GH-alone group showed significantly more mechanical allodynia than the pre-injury data for that group. We had hoped to provide evidence that bFGF – GH could create a better environment for spinal cord regeneration. In the present study, although the bFGF – GH group showed almost identical amounts of recovery in comparison with GH group, we conclude that bFGF – GH created better conditions for decreasing sensory abnormalities.

Conclusion

Although we found few significant effects of bFGF – GH therapy, our results did provide evidence that bFGF-incorporated hydrogel treatment may possibly relieve mechanical allodynia following SCI and should be comparatively safe in future clinical use.

Acknowledgement

This research was supported by a grant-in-aid for Japanese scientific research grant 20591736.

References

1 Furuya T, Hashimoto M, Koda M, Okawa A, Murata A, Takahashi K, *et al.* Treatment of rat spinal cord injury with a Rho-kinase inhibitor and bone marrow stromal cell transplantation. Brain Res 2009;1295:192–202.
2 Marui A, Tabata Y, Kojima S, Yamamoto M, Tambara K, Nishina T, *et al.* A novel approach to therapeutic angiogenesis for patients with critical limb ischemia by sustained release of basic fibroblast growth factor using biodegradable gelatin hydrogel: an initial report of the phase I-IIa study. Circ J 2007;71(8): 1181–6.
3 Iwakura A, Fujita M, Kataoka K, Tambara K, Sakakibara Y, Komeda M, *et al.* Intramyocardial sustained delivery of basic fibroblast growth factor improves angiogenesis and ventricular function in a rat infarct model. Heart Vessels 2003;18(2):93–9.
4 Iwakura A, Tabata Y, Miyao M, Ozeki M, Tamura N, Ikai A, *et al.* Novel method to enhance sternal healing after harvesting bilateral internal thoracic arteries with use of basic fibroblast growth factor. Circulation 2000;102(19 Suppl. 3):III307–11.
5 Aimoto T, Uchida E, Matsushita A, Tabata Y, Takano T, Miyamoto M, *et al.* Controlled release of basic fibroblast growth factor promotes healing of the pancreaticojejunal anastomosis: a novel approach toward zero pancreatic fistula. Surgery 2007; 142(5):734–40.
6 Mattson MP, Lovell MA, Furukawa K, Markesbery WR. Neurotrophic factors attenuate glutamate-induced accumulation of peroxides, elevation of intracellular Ca^{2+} concentration, and neurotoxicity and increase antioxidant enzyme activities in hippocampal neurons. J Neurochem 1995;65(4):1740–51.
7 Kirschner PB, Henshaw R, Weise J, Trubetskoy V, Finklestein S, Schulz JB, *et al.* Basic fibroblast growth factor protects against excitotoxicity and chemical hypoxia in both neonatal and adult rats. J Cereb Blood Flow Metab 1995;15(4):619–23.
8 Anderson KJ, Dam LS, Cotman CW. Basic fibroblast growth factor prevents death of lesioned cholinergic neurons in vivo. Nature 1998;332(6162):360–1.
9 Teng YD, Mocchetti I, Wrathall JR. Basic and acidic fibloblast growth factors protect spinal motor neurons in vivo after experimental spinal cord injury. Eur J Neurosci 1998;10(2):798–802.
10 Itosaka H, Kuroda S, Shichinohe H, Yasuda H, Yano S, Kamei S, *et al.* Fibrin matrix provides a suitable scaffold for bone marrow stromal cells transplanted into injured spinal cord: a novel material for CNS tissue engineering. Neuropathology 2009; 29(3):248–57.
11 Johnson PJ, Tatara A, Shiu A, Sakiyama-Elbert SE. Controlled release of neurotrophin-3 and platelet derived growth factor from fibrin scaffolds containing neural progenitor cells enhances survival and differentiation into neurons in a subacute model of SCI. Cell Transplant 2010;19(1):89–101.
12 Basso DM, Beattie MS, Bresnahan JC. A sensitive and reliable locomotor rating scale for open field testing in rats. J Neurotrauma 1995;12(1):1–21.
13 Mocchetti I, Rabin SJ, Colangelo AM, Whittemore SR, Wrathall JR. Increased basic fibroblast growth factor expression following contusive spinal cord injury. Exp Neurol 1996;141(1):154–64.
14 Zai LJ, Yoo S, Wrathall JR. Increased growth factor expression and cell proliferation after contusive spinal cord injury. Brain Res 2005;1052(2):147–55.
15 Lee YL, Shih K, Bao P, Ghirnikar RS, Eng LF. Cytokine chemokine expression in contused rat spinal cord. Neurochem Int 2000; 36(4–5):417–25.
16 Jimenez Hamann MC, Tator CH, Shoichet MS. Injectable intrathecal delivery system for localized administration of EGF and FGF-2 to the injured rat spinal cord. Exp Neurol 2005; 194(1):106–19.